

AN AUTOMATIC BRANCH AND STENOSES DETECTION IN COMPUTED TOMOGRAPHY ANGIOGRAPHY

Suheyra Cetin[†], Gozde Unal^{**}

Muzaffer Degertekin

Sabanci University

[†]Computer Science and ^{*}Electronics Engineering
Istanbul, Turkey

Yeditepe University Hospital

Department of Cardiology
Istanbul, Turkey

ABSTRACT

In this work, we present an automatic branch and stenoses detection method that is capable of detecting all types of plaques in Computed Tomography Angiography (CTA) modality. Our method is based on the vessel extraction algorithm we proposed in [1], and detects branches and stenoses in a very fast way. We demonstrate the performance of our branch detection method on 3 complex tubular structured synthetic datasets for quantitative validation. Additionally, we show the preliminary results of stenoses detection algorithm on 11 CTA volumes, which are qualitatively evaluated by a cardiologist expert.

Index Terms— stenosis detection, segmentation, CTA, tubular structures, branch detection, vessel trees, coronary arteries

1. INTRODUCTION

In the last decade, CAD (Coronary Artery Disease) has been the leading cause of death worldwide [2]. Extraction of arteries is a crucial step for accurate visualization, quantification, and tracking of pathologies. Especially, early detection and quantification of plaques is of high interest. However, interpreting and detecting the plaques requires substantial experience. It can take several hours for the physicians to do manual plaque segmentation for a single CTA dataset. An automated and fast system that can identify the severe and moderate stenoses could be an alternative to the physicians in the emergency cases.

For the automatic detection of plaques, delineation of coronary arteries is important. Creating a robust fully automatic vessel extraction algorithm is one of the most challenging and ongoing problems in the literature. According to the amount of interaction, methods can be classified into three categories: fully automatic, semi-automatic, or interactive. Fully automatic vessel extraction algorithms, such as [3], implicitly deal with branching. Interactive methods mostly do

not handle branching, since user interaction is provided for every branch. Some semi-automatic methods explicitly represent bifurcations. For instance, Mohan et. al. [4] suggested a K-means clustering algorithm with an assumption that vessels have at most two branches to be separated. Li et. al. [5] proposed to use a 4D interactive key point searching scheme. A comprehensive treatment of the vessel segmentation methods can be found in [6] and [7] surveys.

A variety of algorithms have been proposed in the literature for detection of the plaques in CTA images. However, most of them focus on calcifications, and require substantial user involvement [8]. The most recent work [9] detects and identifies the severe stenoses automatically. However, after the centerline extraction, it requires centerline verification and lumen segmentation steps before stenosis detection.

In this paper, we aim to extract coronary vessel branches from CTA scans and to detect possible abnormalities on arteries. To achieve this goal, we first apply a simple thresholding technique (Section 2.1) as a prefilter to remove calcifications on arteries. Then, we detect the branches in a vessel tree (Section 2.3) based on our vessel extraction method [1] (Section 2.2), which constructs an intensity-based tensor that fits to a vessel, which is inspired from diffusion tensor image (DTI) modeling. Finally, we propose a plaque detection method that can detect all severe plaques in a vessel tree (Section 2.4).

2. METHODS

2.1. Preprocessing

Vessel calcifications are not part of the vessel lumen, for this reason, they are eliminated before applying the vessel tractography algorithm. The images are prepared for segmentation using a thresholding technique by setting the voxel intensity for vessel calcifications equal to the intensity of the myocardial tissue [10].

2.2. Vessel Extraction

In our previous work [1], we designed a novel tensor model for tubular structure segmentation. The anisotropic tensor

^{*}This work was supported by Tubitak - BMBF Germany Bilateral Project no: 108E162.

inside the vessel drives the segmentation analogously to a tractography approach in DTI. Our model is capable of finding vessel orientation, centerline (central lumen line) and its thickness (vessel lumen diameter) at the same time.

2.3. Branch Detection

In order to extend our vessel tractography (VET) model to tubular trees, we propose an unsupervised clustering method, which is capable of detecting *any* number of branchings from a parent coordinate. In our method, we assume that the branches of the vessel tree have similar intensity distributions with the main branch, and have a diameter in a given anatomical range. Our method is initialized with a single seed point and the entire vessel tree can be captured by a non-parametric automatic branch detection algorithm we propose.

First, we search the branches on a spherical surface around the current coordinate. Branch candidate coordinates are calculated as:

$$c(i) = c(u_{n-1}) + 2r\mathbf{g}_i, \quad \mathbf{g}_i \in \mathbf{g} \quad (1)$$

where \mathbf{g} represents orientations on \mathbb{S}^2 , r is a radius parameter, $r \in [r_{min}, r_{max}]$, and $c(u_{n-1})$ is the current centerline coordinate.

2.3.1. Branch Candidate Elimination

We apply three criteria to eliminate the branch candidates that are found by (1):

- (i) We search the branch coordinates in a $\frac{5}{3}\pi$ field of view, which avoids the branch candidates that are already processed.
- (ii) The coordinates, which are out of vessel are eliminated. Mathematically; the intensity mean of the sphere, μ_{sph_1} , centered at the potential branch coordinate, $c(i)$, is defined with a sphere $sph_1 = sph(c(i), r)$, and the intensity mean of the sphere, μ_{sph_0} , centered at the seed, c_{seed} is expressed with $sph_0 = sph(c_{seed}, r_{seed})$. Intensity mean ratio, β , is applied for the potential branch candidates using $\mu_{sph_1} \geq \mu_{sph_0}\beta$. When the potential branch candidate has a mean intensity higher than $\mu_{sph_0}\beta$, the tensor fitting [1] is applied at that coordinate, otherwise it is eliminated. Vessel direction of the branch coordinate, \mathbf{v}_3 , is found as the minor eigenvector of the vessel tensor.
- (iii) Branch candidate coordinates, which have vessel direction that are along the same direction of the current vessel, are eliminated.

Figure 1(a) illustrates the elimination process of branch candidates. Black balls represent the coordinates that are eliminated. On the other hand, red balls are the coordinates that will be clustered.

2.3.2. Clustering of Branch Coordinates

After the branch coordinates are found, vessel direction of the branch coordinates, \mathbf{v}_3 , are used as a feature for clustering. If \mathbf{v}_3 of the tensor of the potential branch coordinate is not in the direction of the current path, \mathbf{v}_3 and its coordinate is put into a new cluster or to an already existing cluster as follows:

- (i) When the vector \mathbf{v}_3 is closer to the directions in one of the previously formed clusters, it is inserted into an appropriate cluster with its corresponding coordinate;
- (ii) When the vector \mathbf{v}_3 has a distinct orientation, a new cluster is constructed, and this vector is added with its corresponding coordinate to that cluster.

Detected branch coordinates and orientation vectors are stacked into clusters. Then, coordinate mean of each cluster is calculated and labelled as a branch coordinate. Figure 1(b) depicts the clustering of branch coordinates (red balls). In the Y-shaped vessel, two branches are found and clustered.

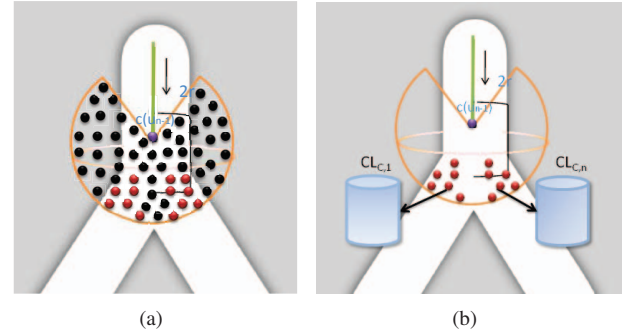


Fig. 1. (a) Branch Elimination process; Black balls: eliminated coordinates, Red balls: coordinates that will be clustered in the next step. (b) Clustering of branch coordinates; Y-shaped vessel splits into two clusters.

2.4. Stenosis Detection

Candidate stenoses regions are identified using the lumen radii, which are estimated during the vessel extraction process.

After the vessel extraction, longitudinal views of each branch are formed for further visualization of stenoses on them. They are created by concatenating the image cuts of the data around the centerline coordinates (Figure 2(a)). Next, we analyze the estimated radius profile and detect possible stenoses regions on arteries. In our stenosis detection algorithm, we mainly focus on the proximal part of the coronary arteries as the diseases are mostly detected in this region. However, since the thickness near to ostium can be anatomically varying, it may lead to wrong detection. So, we discard the part of the vessel until first fall is observed in the radius profile. In other words, we omit the region near to coronary ostium. Possible stenoses regions are the intervals for which

the radius constitutes a valley. To find these regions, first, the estimated radius curve is smoothed by Gaussian filtering (Figure 2(a), blue). Then, we look at the energy profile of the derivative of the radius curve to detect the start and end points of the stenosis. In Figure 2(b), green plot depicts the derivative of the radius profile: (o, +) pairs indicate the start and end points of the stenosis regions. In Figure 2(a), stenotic lesion is indicated by red.

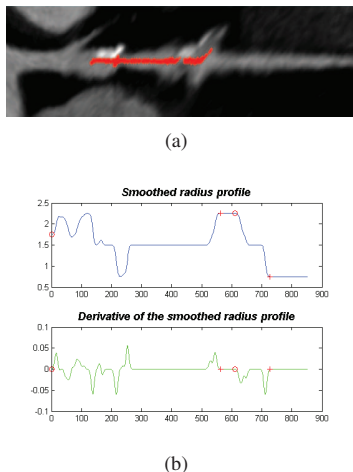


Fig. 2. An example of a CTA data: (a) The presented method detects severe stenoses caused by calcified plaque and non-calcified plaque regions (red); (b) The graphs at the bottom show the smoothed lumen radii estimate (blue) and derivative (green). Detected stenoses regions are depicted by red (o, +) pairs.

3. RESULTS AND EXPERIMENTS

In the first part of this section, we first give a quantitative validation of the performance of our method on 3 synthetic vascular image volumes, which are obtained from the work of Hamarneh and Jassi’s [11] that simulate volumetric images of vascular trees and generate the corresponding ground truth segmentations. Then, we evaluate the performance of our algorithm by adding two levels of salt and pepper noise to three data, and compare our results with the region growing (RG) algorithm. We also analyze the performance of our algorithm by adding Gaussian noise with two different variances. For each case, a single seed point is selected from each tree, then entire vessel tree is segmented automatically. We used 128 unit directions, \mathbf{g} , on S^2 and the radius range is selected between 0.25 and 4 mm. Additionally, β , ratio of intensity mean of the spheres is heuristically set to 0.85 for all experiments. In the second part, we first evaluate our stenoses detection method on synthetic varying cylinder dataset [12]. At last, we show the qualitative performance of our method on real CTA data.

3.1. Branch Detection

As the performance of whole vessel tree segmentation correlates directly with branch detection, we show the overlap-like measures of the segmentation map here. We used four different quantitative measures for the synthetic validation as TP (True Positive), FN (False Negative), FP (False Positive) and OM (Overlap Measure) between the estimated vessel map and the ground truth vessel map. Table 1 shows the comparison of the region growing algorithm with our method. Our algorithm is more resistive to salt and pepper noise compared to region growing algorithm. Table 2 shows the performance analysis of our method in the presence of two levels of Gaussian noise: $\sigma_{noise}^2 = 20$, $\sigma_{noise}^2 = 60$. As it is seen from the results, the algorithm is able to detect correctly most of the vessel structures and branches in all cases.

Table 1. Comparisons of the segmentation results of our method (VET) with the region growing (RG): additional salt & pepper noise with weights of 0.05 and 0.2.

	Measure (%)	data 1		data 2		data 3	
		RG	VET	RG	VET	RG	VET
Weight=0.05	TP	66.28	93.28	65.91	94.02	69.91	94.91
	FN	33.72	6.72	34.09	6.08	30.09	5.09
	FP	0.19	8.83	0.20	6.09	0.63	5.33
	OM	79.63	92.31	79.35	93.97	82.28	94.80
Weight=0.2	TP	63.02	92.04	48.92	93.21	60.10	93.54
	FN	36.98	7.96	51.08	6.79	39.90	6.46
	FP	1.22	8.91	0.60	6.13	0.17	5.82
	OM	76.74	91.60	65.44	92.35	74.99	92.49

Table 2. Performance analysis of our method in the presence of two levels of Gaussian noise: $\sigma^2 = 20$, $\sigma^2 = 60$.

Measure (%)	data 1		data 2		data 3	
	$\sigma^2 = 20$	$\sigma^2 = 60$	$\sigma^2 = 20$	$\sigma^2 = 60$	$\sigma^2 = 20$	$\sigma^2 = 60$
TP	92.89	90.65	93.78	91.43	94.23	92.28
FN	7.11	9.35	6.22	8.57	5.77	7.72
FP	8.45	8.97	6.73	7.92	6.13	6.86
OM	92.27	90.82	93.54	91.73	94.06	92.76

Figure 3 depicts the result of our algorithm on one of the three synthetic vascular dataset from Hamarneh and Jassi’s work [11] with additional salt and pepper noise by 0.2 weight. Extracted centerline of the dataset is shown by green. Vessel tree with radial thickness is shown by orange on the right.

3.2. Stenosis Detection

We first tested our algorithm on synthetic, contrast and radii varying dataset. Detected stenosis region of the volume is depicted by red (Figure 4). Then, we apply our algorithm on 11 CTA volumes to detect calcifications, mixed plaques and soft plaques; and the results are evaluated by a cardiologist expert visually. Figure 5 depicts the application of our method to three different cases. In all cases, our method can locate all severe stenotic lesions correctly.

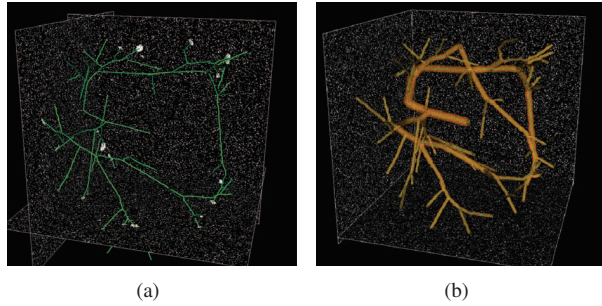


Fig. 3. Extracted vessel tree from the $101 \times 101 \times 101$ synthetic vascular dataset with salt and pepper noise of weight 0.2.

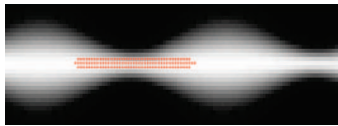


Fig. 4. An example of a stenosis detection: Synthetic vessel volume with varying radius, detected stenosis region is depicted by red.

4. CONCLUSION

In this paper, an automatic method for the detection of branches of arteries and stenotic lesions in CTA is proposed. We demonstrated the performance of our branch detection method quantitatively on 3 complex tubular structured synthetic datasets. Additionally, detected stenoses on 11 CTA volumes were shown for qualitative validation of the method. Further extensive validation studies of stenoses detection will be carried out and presented in the next phase of this work.

5. REFERENCES

- [1] S. Cetin, G. Unal, A. Demir, and M. Degertekin, "Vessel tractography using an intensity based tensor model," *The MICCAI Workshop on CVII*, 2011.
- [2] WHO, "The 10 leading causes of death by broad income group (2004)," *World Health Organization Media Center, editor*, October 2008.
- [3] S. Zambal, J. Hladuvka, A. Kanitsar, and K. Buhler, "Shape and appearance models for automatic coronary artery tracking," *In MICCAI 2008 Contest: 3D Segmentation in Clinic: A Grand Challenge*, 2008.
- [4] Vandana M., Ganesh S., and Allen T., "Tubular surface segmentation for extracting anatomical structures from medical imagery," *IEEE Trans. Med. Imag.*, pp. 1945–1958, 2010.

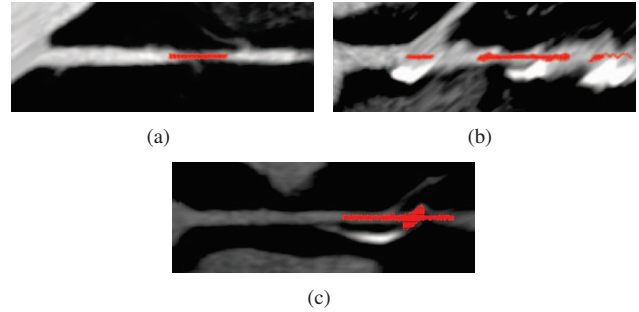


Fig. 5. Stenoses labeling are shown by red: (a) soft plaque, (b) calcifications, (c) mixed plaque.

- [5] H. Li, A. Yezzi, and L. Cohen, "3d multi-branch tubular surface and centerline extraction with 4d iterative key points," in *MICCAI '09: Part II*, Berlin, Heidelberg, 2009, pp. 1042–1050, Springer-Verlag.
- [6] C. Kirbas and F. Quek, "A review of vessel extraction techniques and algorithms," *ACM Comput. Surv.*, vol. 36, pp. 81–121, June 2004.
- [7] D. Lesage, E.D. Angelini, I. Bloch, and G. Funka-Lea, "A review of 3D vessel lumen segmentation techniques," *Med. Imag. Anal.*, vol. 13, no. 6, pp. 819–845, Dec. 2009.
- [8] S. Wesarg, M. Khan, and E. Firlre, "Localizing calcifications in cardiac ct data sets using a new vessel segmentation approach," *Journal of Digital Imaging*, vol. 19, pp. 249–257, 2006.
- [9] B. M. Kelm, S. Mittal, Y. Zheng, and et al., "Detection, grading and classification of coronary stenoses in computed tomography angiography," in *MICCAI'11: Part III*, Berlin, Heidelberg, 2011, pp. 25–32, Springer-Verlag.
- [10] Ola Friman, Milo Hindennach, Caroline Kühnel, and Heinz-Otto Peitgen, "Multiple hypothesis template tracking of small 3D vessel structures," *Med. Imag. Anal.*, vol. 14, no. 2, pp. 160–171, Apr. 2010.
- [11] G. Hamarneh and P. Jassi, "Vascusynth: Simulating vascular trees for generating volumetric image data with ground-truth segmentation and tree analysis," *Computerized Medical Imaging and Graphics*, vol. 34, no. 8, pp. 605 – 616, 2010.
- [12] Karl Krissian and Gr Malandain, "Synthetical test images for vascular segmentation algorithms," <http://lmi.bwh.harvard.edu/research/vascular/SyntheticVessels/SyntheticVesselImages.html>.